Postpartum Cervical Repair In Mice: A Morphological Characterization And Potential Role For Angiogenic Factors

By: **Chishimba Mowa**, Takako Ohashi, & Robert Stanley

Abstract

The cervix undergoes marked mechanical trauma during delivery of the baby at birth. As such, a timely and complete tissue repair postpartum is necessary to prevent obstetrical complications, such as cervicitis, ectropion, hemorrhage, repeated miscarriages or abortions and possibly pre-term labor and malignancies. However, our knowledge of normal cervical repair is currently incomplete and factors that influence repair are unclear. Here, we characterize the morphological and angiogenic profile of postpartum repair in mice cervix during the first 48 h of postpartum. The key findings presented here are: (1) cervical epithelial folds and size are diminished during the first 48 h of postpartum repair, (2) hypoxic inducible factor 1a, vascular endothelial growth factor (VEGF), and VEGF receptor 1 expression are pronounced early in postpartum cervical repair, and (3) VEGF receptor 2 gene and protein expressions are variable. We conclude that postpartum cervical repair involves gross and microscopic changes and is linked to expression of angiogenic factors. Future studies will assess the suitability of these factors, identified in the present study, as potential markers for determining the phase of postpartum cervical repair in obstetrical complications, such as cervical lacerations.

Chishimba, Mowa & Takako, Ohashi & Stanley, Robert (2015) "Postpartum Cervical Repair In Mice: A Morphological Characterization And Potential Role For Angiogenic Factors " *Cell and Tissue Research* vol. 362 issue. 1 pp. 253-263 [DOI: 10.1007/s00441-015-2184-x]
Version of Record Available @ www.springer.com

Introduction

The cervix undergoes marked changes during pregnancy, as well as significant trauma during normal vaginal delivery of the baby at birth (parturition) and immediately postpartum (after birth) (Timmons et al. 2010). As such, a timely and complete postpartum tissue repair is necessary to prevent obstetrical complications, such as cervicitis, ectropion, hemorrhage, repeated miscarriages or abortions and, possibly, preterm labor and malignancies (Fahmy et al. 1991). For instance, during pregnancy, the cervix has to contain and withstand an ever increasing gravitational force exerted by the rapidly growing fetus in order to ensure that it (the fetus) is held in utero (Timmons et al. 2010), whereas at parturition, under the intense force of the contracting uterus, the ripened cervical tissue is forced to expand and dilate to ultimately allow passage of the fetus through the birth canal (Mahendroo 2012). Immediately following these dramatic mechanical tissue "assaults", the cervix undergoes an extensive postpartum reconstruction and healing phase that restores it (the cervix) to its non-pliable non-pregnant state (Timmons and Mahendroo 2007). Collectively, these changes (gestational and postpartum) are termed cervical remodeling (CR), which is divided into four distinct yet overlapping phases, namely softening, ripening, dilation and postpartum repair (Read et al. 2007; Word et al. 2007). To date, most of the studies have focused on the first three phases of CR, almost at the exclusion of postpartum repair.

Postpartum repair consists of a set of complex biological processes that ultimately restores the cervix to its original non-pregnant state, and thus ensures normal cervical function for subsequent pregnancies (Timmons et al. 2010; Mahendroo 2012). This final phase of CR is generally characterized as an inflammatory and wound-healing response (Timmons and Mahendroo 2007; Bauer et al. 2009), as demonstrated by

studies that utilized gene microarrays. These studies have shown that a variety of factors, including pro-inflammatory factors, metalloproteases, proteins involved in extracellular matrix (ECM) synthesis, and genes governing epithelial differentiation pathways are all up-regulated postpartum (Timmons and Mahendroo 2007; Gonzalez et al. 2009). Immune cells, including neutrophils, eosinophils, and both M1 and M2 macrophages, have all been shown to increase postpartum compared to earlier phases of remodeling (Timmons et al. 2009, 2010; Mahendroo 2012). This inflammatory response could serve to promote repair of the cervix after parturition and/or serve a protective role of the birth canal against environmental hazards, such as infection (Gonzalez et al. 2009). Because inflammation and wound healing are intricately linked to vascular events, factors that regulate this process, notably vascular endothelial growth factor (VEGF) (Nguyen et al. 2012), also likely influence postpartum cervical repair. Of note, VEGF is expressed in normal, pregnant and cancerous cervices in rodents and humans.

The importance of the role of VEGF in wound healing has been well documented and characterized (Galiano et al. 2004; Mowa et al. 2008a; Alberts et al. 2008; Bao et al. 2009). VEGF controls wound healing by inducing various vascular processes, including angiogenesis (capillary growth), vasopermeability, and recruitment of immune cells, as well as epithelization and collagen deposition (Bao et al. 2009), the hallmark of the healing response (Mahendroo 2012). For instance, induction of capillary growth during wound repair meets the growing demands for oxygen and nutrients, as well as removal of waste products (Alberts et al. 2008). Indeed, inhibition of angiogenesis impairs wound healing, demonstrating the vital role of VEGF in this (healing) process (Galiano et al. 2004; Bao et al. 2009). Factors that induce VEGF expression during wound healing include growth factors (transforming growth factor, hepatocyte growth factor, keratinocyte growth factor, etc.), pro-inflammatory cytokines, such as interleukin-1 (IL-1) and tumor necrosis factor alpha (TNFα), and, notably, hypoxia, i.e., low oxygen (Eming and Krieg 2006). Cells in a hypoxic environment will accumulate the intracellular transcription factor, hypoxia inducible factor-1 alpha (HIF-1α), which is the most potent inducer of VEGF transcription (Majmundar et al. 2010). Following injury, VEGF is first secreted by hypoxic cells and will establish a gradient of VEGF, mirroring the gradient of hypoxia (Alberts et al. 2008). Activated platelets, and immune cells, i.e. macrophages and neutrophils, express VEGF receptor 1 (VEGFR1) and respond chemotactically to VEGF, and will migrate towards the VEGF source at the site of injury and/or hypoxia (Bao et al. 2009; Eming and Krieg 2006). Macrophages and neutrophils will in turn stimulate angiogenesis by further secreting VEGF and TNFα that will also stimulate VEGF production in keratinocytes and fibroblasts (Bao et al. 2009). Although the role of VEGF in the cervical events during pregnancy has been studied (Nguyen et al. 2012; Eming and Krieg 2006; Mowa et al. 2004, 2008b; Donnelly et al. 2013), to date, no study has examined its role, if any, in postpartum cervical repair.

The presence and profile of VEGF and its key tyrosine kinase receptors have been characterized in the uterine cervix of rodents (mice and rats), and human and VEGF-related genes in rats have been delineated using DNA microarray analysis in pregnant and non-pregnant conditions (Nguyen et al. 2012; Mowa et al. 2004, 2008a, b; Donnelly et al. 2013; and unpublished data). The effects of VEGF are largely mediated by VEGFR-1 (or fms-related tyrosine kinase-1, flt-1) and VEGF R-2, which have different signaling properties and are largely expressed by endothelial cells (Mowa et al. 2004).

Since postpartum repair is considered a pro-inflammatory wound healing response (Mahendroo 2012; Timmons and Mahendroo 2007; Bao et al. 2009), and VEGF is known to induce inflammation in the cervix (Nguyen et al. 2012) and plays roles in: (1) cervical remodeling (CR) during pregnancy in rodents (Mowa et al. 2008b; Donnelly et al. 2013), and (2) general wound healing (Bao et al. 2009; Eming and Krieg 2006), here we speculate that VEGF plays a role in the postpartum repair phase of CR. In this study, we sought to determine: (1) the gross morphological changes of the postpartum cervix, and (2) the expression patterns of HIF-1α, VEGF, and the VEGF receptors (VEGFR-1 and VEGFR-2), during the first 2 days in mice.

Materials and methods

Animals and postpartum time intervals

Pregnant mice (C57BL6/129SvEv; Charles River, n=3~5 per technique of each time-point, except for H&E staining and confocal immunofluorescence, where n=1) were used in the present study during the time points specified here: The time of the first pup was noted as time 0 h and the mothers were sacrificed at an 8-h interval, after parturition, beginning with 0 h, i.e., 0, 8, 16, 24, 32, 40 and 48 h. The average interval between the birth of the first and last pup was within 1 h, with an average litter size between 8–12 pups. All animals were euthanized by a lethal injection of sodium pentobarbital (150 mg/kg bw, i.p.) and transcardially perfused with 0.9 % saline solution. Cervices were carefully harvested under a stereomicroscope, to avoid contamination with vaginal and uterine tissues, and the tissues were then processed and analyzed accordingly, including using scanning electron and light microscopy imaging, gene expression analysis using real-time PCR, and protein expression analysis using Western blot and confocal immunofluorescence. All animals were housed under the following conditions: constant room temperature (RT); a 12:12-h light:dark cycle, and free access to water and food. All experiments were performed in accordance with the

Institutional Animal Care and Use Committee (IACUC) of Appalachian State University and the NIH guidelines (NIH publication number 86-23), with efforts made to minimize both number of animals used and animal suffering.

Scanning electron microscopy (SEM)

SEM was employed to observe the surface of cervical epithelia and any changes occurring during the postpartum period.

Harvested cervices were immediately immersed in a 2.5 % glutaraldehyde, 0.1 M phosphate buffer solution (PBS) and the tissues were then dehydrated in a graded series of ethanol and dried using a critical point drying apparatus (Polaron Instruments, Laughton, East Sussex, UK). The dry samples were mounted on aluminum stubs with carbon adhesive paper, sputter-coated in gold and viewed with the SEM (FEI, Hillsboro, OR, USA). The cervical epithelium was evaluated for various features, including, but not limited to, involutions, tissue size, overall appearance of cells, presence of macrophages and paracellular spaces.

Confocal immunofluorescence

Confocal immunofluorescence was employed to complement Western blot data of the proteins of interest (VEGF, VEGF receptors, HIF-1α), as well as determine their cellular localization in the cervix.

Harvested cervices were immersed in a 10 % formalin (pH 7.2) aqueous solution. The tissues were fixed in formalin at 4 °C for 3–4 days and then transferred into saturated sucrose dissolved in 0.1 M PBS, for at least 2 days prior to sectioning (12 μm) with the Cryostat (Leica, Buffalo Grove, IL, USA) at −30 °C. After sectioning, the slides were either stained immediately or stored at –20 °C until staining. For staining, the sections were initially incubated with 10 % normal goat serum in 0.1 M PBS for 20 min at RT in order to block non-specific protein binding. Next, the sections were washed 3 times in 0.1 M PBS and then incubated overnight at 4 °C with diluted primary antibodies of interest at 0.5 μg/mL (Santa Cruz Biotech, Santa Cruz, CA, USA). The next day, the sections were washed 3 times with 0.1 M PBS Buffer followed immediately by incubation in diluted fluoro-tagged secondary antibody at 0.5 μg/mL (Santa Cruz Biotech) for 1 h at RT. Thereafter, the sections were washed 3 times with 0.1 M PBS, counterstained with 5 μM Sytox Green™, mounted with aqueous Ultracruz Mounting Medium (Santa Cruz Biotech), and then examined with a confocal microscope (Carl Zeiss, Peabody, MA, USA).

Gene expression studies (real time PCR)

To perform gene expression studies, total RNA was first extracted, reverse-transcribed into cDNA and then amplified. Harvested cervices were snap-frozen and then either total RNA was extracted immediately or the tissues were stored at −80 °C until processing. Tissues were first homogenized in Qiazol Lysis reagents (Qiagen, Valencia, CA, USA) and then total RNA was extracted using RNeasy Mini Kit (Qiagen) and its quality and quantity determined using the Nanodrop apparatus (Thermo Scientific, Waltham, MA, USA). If of good quality and quantity, the total RNA (1000 ng) was then reverse transcribed using a cocktail containing the following: $MgCl_2$, reverse transcriptase, RT buffer, dNTP, RNase inhibitor, RNase-free water and random hexamers, in order to generate an equivalent amount of total cDNA using a thermocycler (Eppendorf, Hamburg, Germany) at the following settings: 25 °C for 10 min, 42 °C for 2 h, 95 °C for 5 min, and 4 °C for storage, according to protocol. The cDNA was then used to amplify specific gene sequences using real-time PCR amplification (e.g., VEGF, VEGFR1, VEGFR2, HIF-1α, and Gus-β as a normalizer) in order to determine the relative expression of these genes in all the time points during the 48 h after the onset of parturition. We used commercially predesigned and optimized real time PCR probes (Applied Biosystems, Carlsbad, CA, USA). The PCR reactions were set up in 96-well plate in a volume of 25 μl per well, with the following components: 1 μl of cDNA, 12.5 μl of 2× Taqman Universal PCR Mastermix, 1.25 μl of 20× Assays-on-demand Gene Mix (e.g. VEGF), and 10.25 μl of RNase-free water. DNA amplification was performed using the ABI 7300 HT Real-Time PCR machine (Applied Biosystems. Carlsbad, CA, USA) with the GeneAmp 7300 HT sequence detection system software (Perkin-Elmer, Waltham, MA, USA), with the settings as follows: 95 °C for 10 min, and then 40 cycles of 95 °C for 15 s, and 60 °C for 60 s.

Western blot analysis

Western blot analysis was used to confirm relative amounts of the proteins of interest, at the tissue level.

Harvested cervices were snap-frozen and stored at −80 °C until processing. Total protein was extracted using the protein inhibitor cocktail and Cell Lysis buffer (Sigma Aldrich, St. Louis, MO, USA), and quantified with a bicinchoninic acid (BCA) assay (Thermo Scientific). Next, 10 μg of protein samples, along with a set of standard protein ladders (Bio-Rad, Hercules, CA, USA), were loaded on a 4-12 % Bis-Tris Gel (Invitrogen, Waltham, MA, USA). The gel was electrophoresed at 75 V until the dye was close to the bottom of the gel. Thereafter, the protein was transferred to a PVDF membrane using the iBlot apparatus (Invitrogen, Waltham, MA, USA), and the membrane was incubated overnight with Blotto (5 % dehydrated milk in Tris Buffered Saline with Tween) solution at 4 °C. The following day, the membrane was incubated with the diluted primary antibody dissolved in Blotto (Santa Cruz Biotech), and left to incubate overnight on

a shaker at RT. Thereafter, the membrane was washed three times in 1× TBST for 20 min, after which the membrane was incubated with the diluted secondary antibody, i.e., donkey anti-rabbit IgG HRP conjugated and StrepTactin HRP antibodies (Santa Cruz Biotech) for 1 h at RT on a shaker. The membrane was then washed three times with 1× TBST and one wash with 1× TBS. Horseradish peroxidase solution (Bio-Rad) was added to the membrane for 5 min and the excess solution was dripped off. The membranes were then exposed to x-ray film (GE, Fairfield, CT, USA) in a dark room for an optimal period (~30 s–1 min), and the film was developed and analyzed for presence of the target proteins (VEGF, VEGFR1, VEGFR-2, HIF-1α, and β actin as a normalizer). The densitometry was quantified using ImageJ software (NIH, Bethesda, MD, USA).

Statistical analysis

Data for western blot and real-time PCR analyses were analyzed using Student's *t* test and ANOVA, followed by Scheffe's *F* test for multiple comparisons. *P* values of <0.05 were considered to be statistically significant.

Results

The murine cervix undergoes pronounced morphological changes during the first 48 h postpartum

SEM analysis of cervices obtained from mice at 0, 24, and 48 h postpartum displayed distinct morphological features at the time points of interest (Fig. 1). At 0 h, the cervical epithelium displayed folds (Fig. 1a, b) and micro-folds (Fig. 1c, d), as well as less prominent epithelial cell borders, compared to both 24- and 48-h postpartum. A layer of unidentified extracellular matrix or cell debris appeared at 24 h postpartum (Fig. 1g, h), but disappeared by 48 h postpartum. At both 24- and 48-h postpartum, the presence of "pits" or gaps in the cervical epithelium was observed and the cell–cell borders were more pronounced than at 0 h (Fig. 1f, g, j, k). In order to further characterize the morphological changes of the postpartum cervix, we performed H&E staining, which revealed folded cervical epithelium at 0 h PP (Fig. 2a). At 24 h PP, the layer of unidentified cellular debris reported earlier under SEM data was observed (Fig. 2d), but not at 48 h PP (Fig. 2g), consistent with the SEM findings.

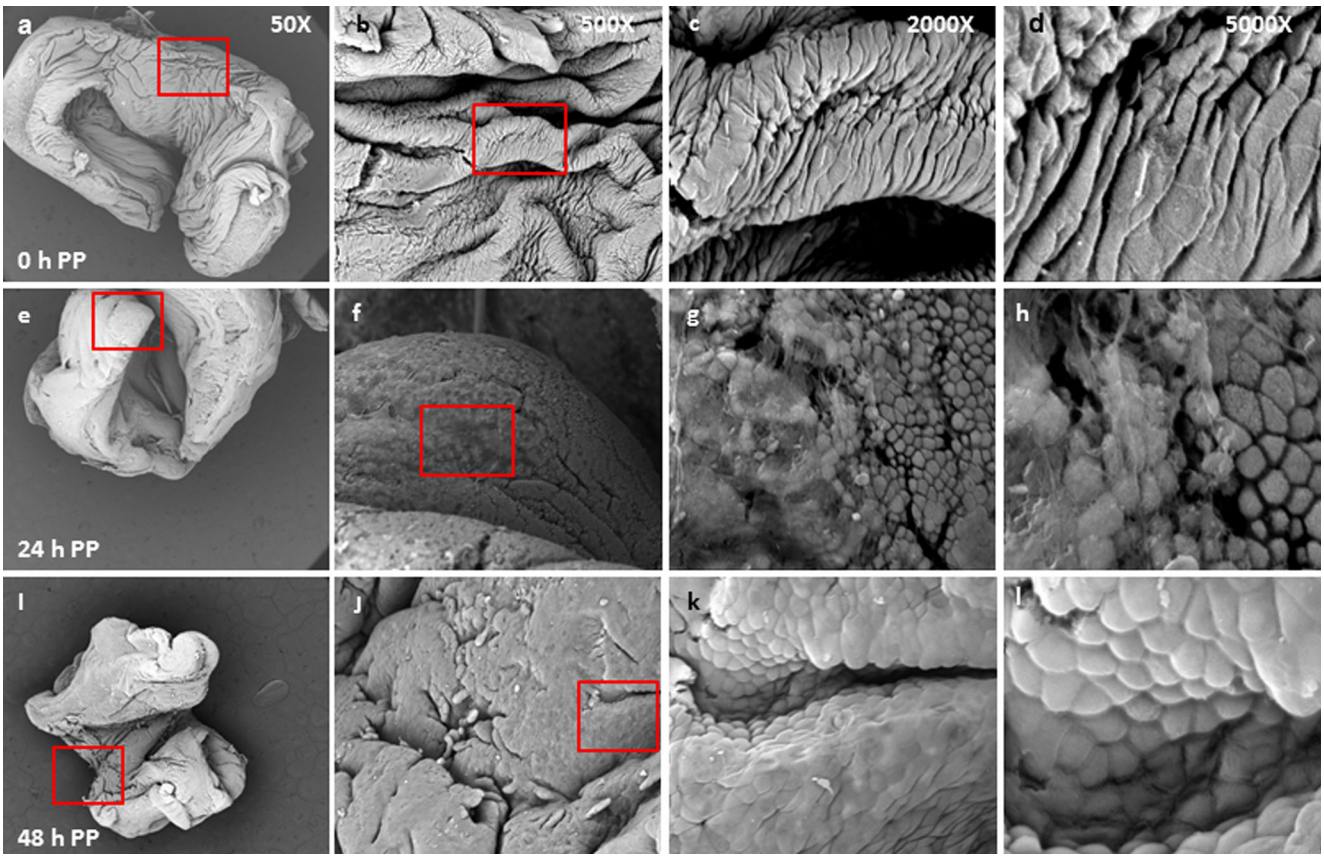

Fig. 1 Scanning electron microscopy images of the chronological profile of postpartum mouse cervical tissue. Low magnification (×50) images reveal an obvious decrease in size from 0 to 48 h postpartum (PP) (**a, e, i**). Cervical epithelial folds, as well as diminished cell–cell borders, were prominent at 0 h PP at higher magnifications (×500–×5,000). An unidentified "covering" was observed at 24 h PP, but was absent at 0 h and had disappeared by 48 h PP. $n=3$

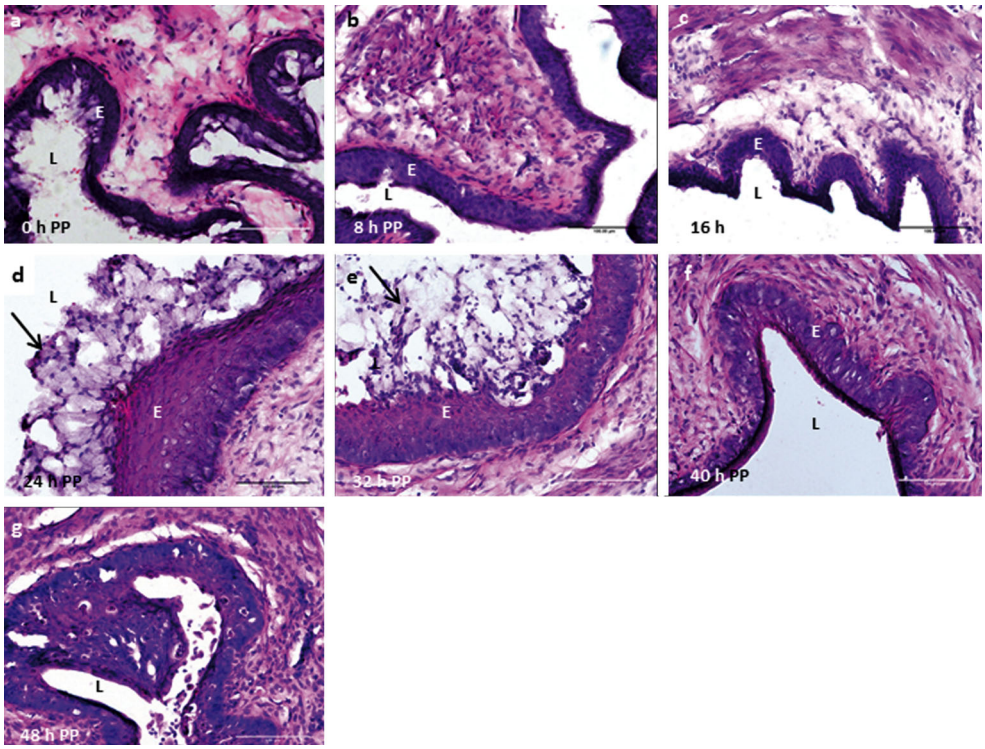

Fig. 2 Histological images of mouse postpartum (PP) cervical tissue, as revealed by H&E staining. During the hours after parturition [0 h postpartum (PP)], the cervical tissue had stromal cells that appeared more dispersed, likely due to edema, in the first 24 h PP (**a**–**d**) but disappeared thereafter (**e**–**g**). At 24 and 32 h PP, a layer of unidentified cellular debris (*arrows*) was observed. *E* cervical epithelium, *L* cervical lumen. All images were taken at ×20. $n=1$

Gene expression in the murine cervix postpartum

Both VEGFR-1 and VEGFR-2 relative mRNA expressions were elevated at 0 h postpartum, with approximately 17- and 9-fold increases, respectively, but declined significantly by 48 h postpartum to non-pregnant levels (Fig. 3). VEGF mRNA expression displayed a 13-fold increase at 0 h postpartum compared to non-pregnant animals, with decreased expression at 48 h postpartum relative to 0 h postpartum, but elevated compared to non-pregnant (Fig. 3). HIF-1α displayed a similar expression pattern, with an 11-fold increase at 0 h postpartum compared to non-pregnant state, followed by a significant decrease in expression by 48 h postpartum, relative to 0 h postpartum, and only slightly elevated compared to non-pregnant (Fig. 3).

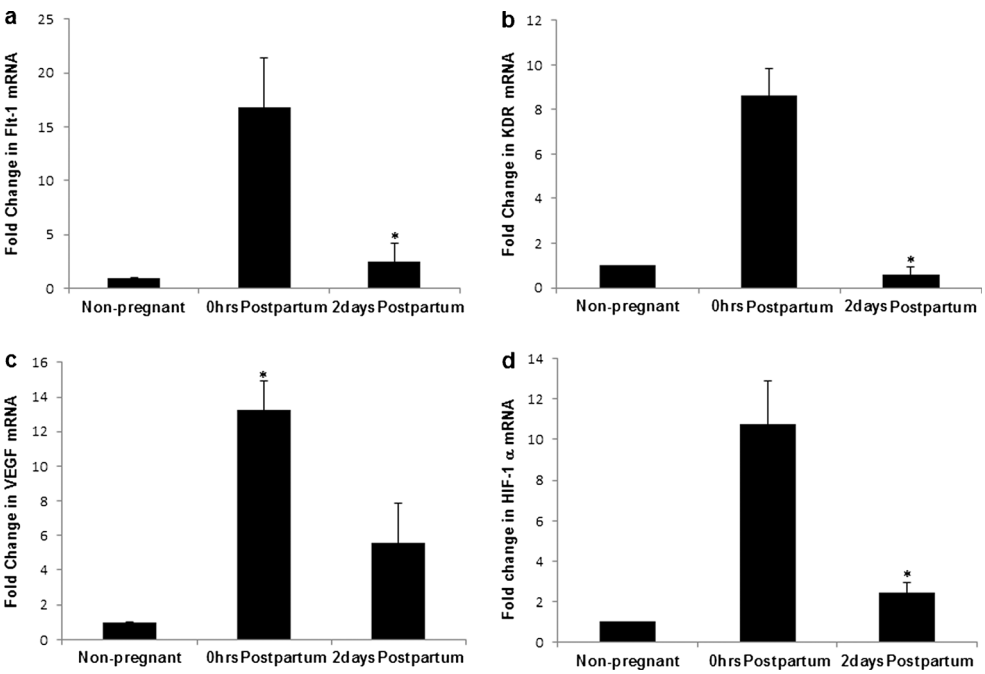

Fig. 3 Gene expression of angiogenic factors {VEGF, VEGF receptors [Flt-1, VEGFR-2 (KDR)] and HIF-1α} in the postpartum (PP) mouse cervix, as revealed by real-time PCR analysis. All the genes of interest were highly expressed at 0 h PP, decreasing significantly by 48 h PP for HIF-1α (*p value=0.02) (**d**), VEGFR-2 (*p value=0.008) (**b**) and Flt-1 (*p value=0.04) (**a**) relative to 0 h. VEGF expression decreased at 48 h PP but was not found to be significant and was several folds above the control (non-pregnant animals) (**c**). $n=5$

Protein expression in the mouse cervix postpartum

VEGF protein expression was found to be at the highest level at 0 h postpartum, with levels decreasing approximately 2 fold by 16 h postpartum, followed by a slight decrease for the remaining time intervals (Fig. 4a). VEGFR-1 was found to be at its highest expression at 8 h postpartum, with levels decreasing in the remainder of time intervals, save for a slight increase at 24 h postpartum, relative to 16 h postpartum (Fig. 4d). It should be noted that the fold change from the highest expression (8 h postpartum) to the lowest expression (48 h) was less than half. In contrast, the other receptor VEGF R-2, was found to increase steadily during the postpartum time intervals; with the lowest levels at 0 h, steadily increasing thereafter and leveling off at 40-48 h postpartum (Fig. 4c). HIF-1α protein expression pattern was similar to VEGF, i.e., it was elevated at 0 h postpartum, and was at its lowest at 48 h postpartum (Fig. 4b). However, there was an increase in expression from 16 to 24 h postpartum, remaining elevated at 32 h, and falling off again by 40 h postpartum (Fig. 4b).

Protein expression in the mouse cervix postpartum, as revealed by confocal immunofluorescence

The highest levels of VEGF were observed at 0 h postpartum (Fig. 5a), with the lowest levels occurring at 48 h postpartum (Fig. 5g). The most pronounced expressions of VEGF were localized on the apical side of the epithelium, regardless of the time interval or point. It is noteworthy that the expression of VEGF was readily detected in the layer of cell debris observed at 24 h postpartum (Fig. 5d) and 32 h postpartum (Fig. 5e). HIF-1α expression mirrored that of VEGF, i.e., the highest levels were at 0 h postpartum (Fig. 5a), lowest at 48 h (Fig. 5g), with expression preferentially localized at the apical side of the cervical epithelium at each time interval. Also, HIF-1α expression was similar to VEGF in that it was also readily expressed in the layer of cell debris at 24 h postpartum (Fig. 5d) and 32 h postpartum (Fig. 5e). The VEGF receptors demonstrate different patterns of expression postpartum. VEGFR-1 expression mirrored that of VEGF and HIF-1α, with expression clearly at its highest at 0 h postpartum (Fig. 6a), lowest at 48 h postpartum (Fig. 6g), and localized to the apical side of the epithelium and in the cell debris layer at both 24 h postpartum (Fig. 6d) and 32 h postpartum (Fig. 6e). Overall, intensity of VEGFR-2 immunostaining increased over time, particularly from 16 h postpartum in epithelia and stromal cells, with the weakest signal appearing between 0-8 h and slightly diminishing at 48 h (Fig. 7) (Fig. 8).

Discussion

Of the four phases of cervical remodeling, postpartum repair is the least studied and, to date, there has been no comprehensive study that has focused exclusively on this fourth and final phase of cervical remodeling. A comprehensive knowledge

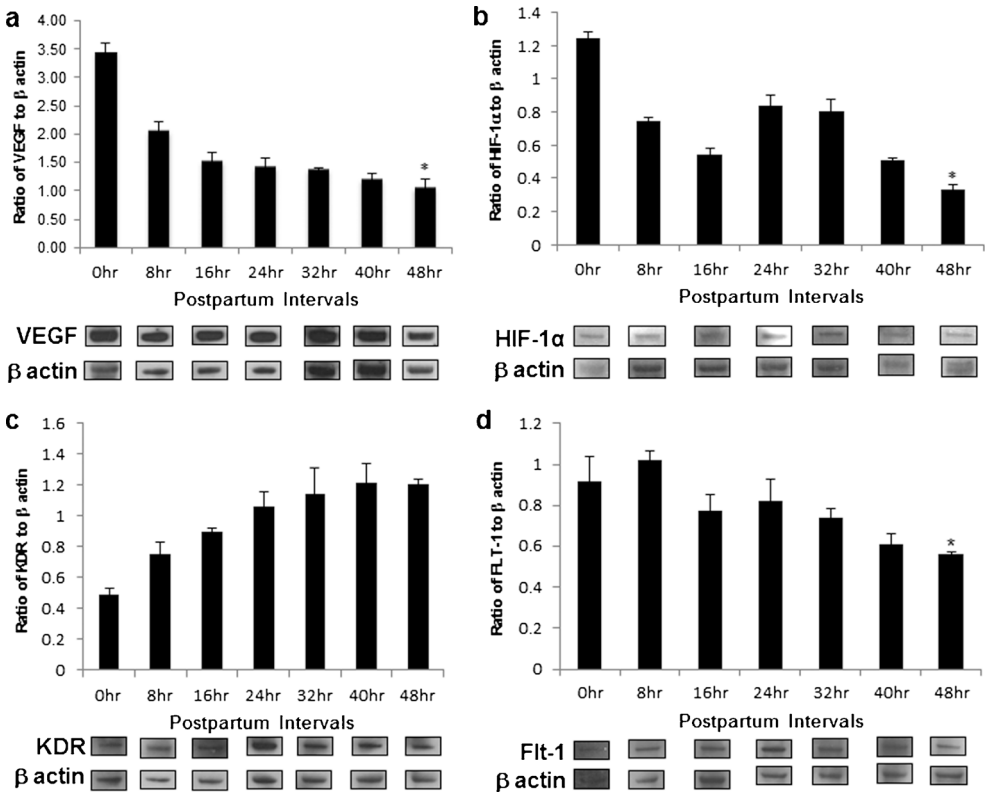

Fig. 4 Chronological expression patterns of VEGF, HIF-1α, Flt-1, and VEGFR-2 (KDR) proteins in postpartum mouse cervix, as determined by Western blot analysis. **a** VEGF protein expression decreased over time between 0 and 48 h postpartum (PP) (*p value=4.56 × 10^{-8}); **b** HIF-1α protein expression decreased between 0 and 16 h but surged to 8 h levels between 24 and 32 h, and decreased steadily thereafter, reaching its lowest levels by 48 h PP (*p value= 3.08 × 10^{-8}); **c** VEGFR-2 protein expression pattern was opposed to that of VEGF, i.e., it steadily increased over time, plateauing by 40–48 h PP (*p value=0.0005); and **d** Flt-1 protein expression pattern overall showed a similar pattern to VEGF, i.e., decreased steadily between 0 and 48 h PP (*p value=0.008). β actin was used as the normalizer. n=5

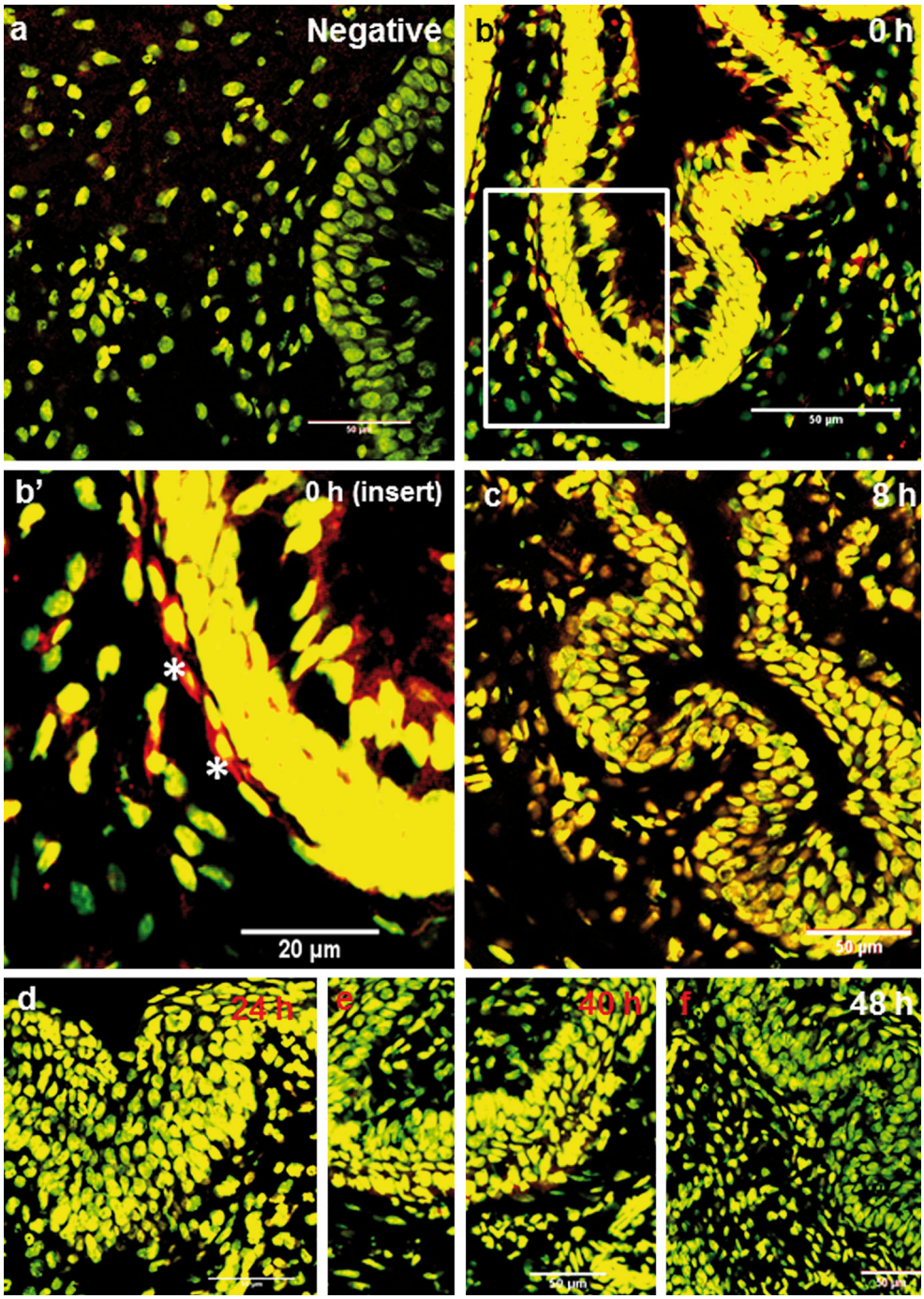

Fig. 5 Chronological cellular expression pattern of VEGF in postpartum mouse cervix, as revealed by confocal immunofluorescence. VEGF immune-expression was initially concentrated in cervical epithelia cells (**b**, **b'**, 0 h), spreading later to the other cell types (stromal) (**c**, 8 h) and diminishing in intensity by 24 h and thereafter (**d**–f). The sections were stained with VEGF Texas red antibodies and a nuclei-specific stain, i.e., Sytox Green™, which stains *green*. The overlap between the two appears as *yellow*. $n=1$

of this phase of CR is potentially vital as it may improve our understanding of obstetrical complications that may be associated with this period, such as cervicitis, ectropion, hemorrhage, repeated miscarriages or abortions and, possibly, preterm labor and malignancies (Fahmy et al. 1991). The present study is the first comprehensive postpartum study and uses a variety of techniques to examine the morphological and molecular changes in the mouse cervix during the first 48 h of postpartum. The key findings of the present data are: (1) epithelial folds and cervical size progressively diminish during postpartum repair, (2) HIF-1α, VEGF, and VEGFR-1 expression are pronounced early in postpartum cervical repair, and (3) VEGFR-2 gene and protein expressions are variable.

The current SEM data show the presence of cervical epithelial folds at 0 h postpartum. These findings are consistent with our most recent work that utilized SEM and bromodeoxyuridine (BrdU) staining showing cervical epithelial proliferation leading up to parturition, as well as in non-pregnant ovariectomized mice that were treated with exogenous VEGF (Mowa et al. 2008b; Donnelly et al. 2013). Of

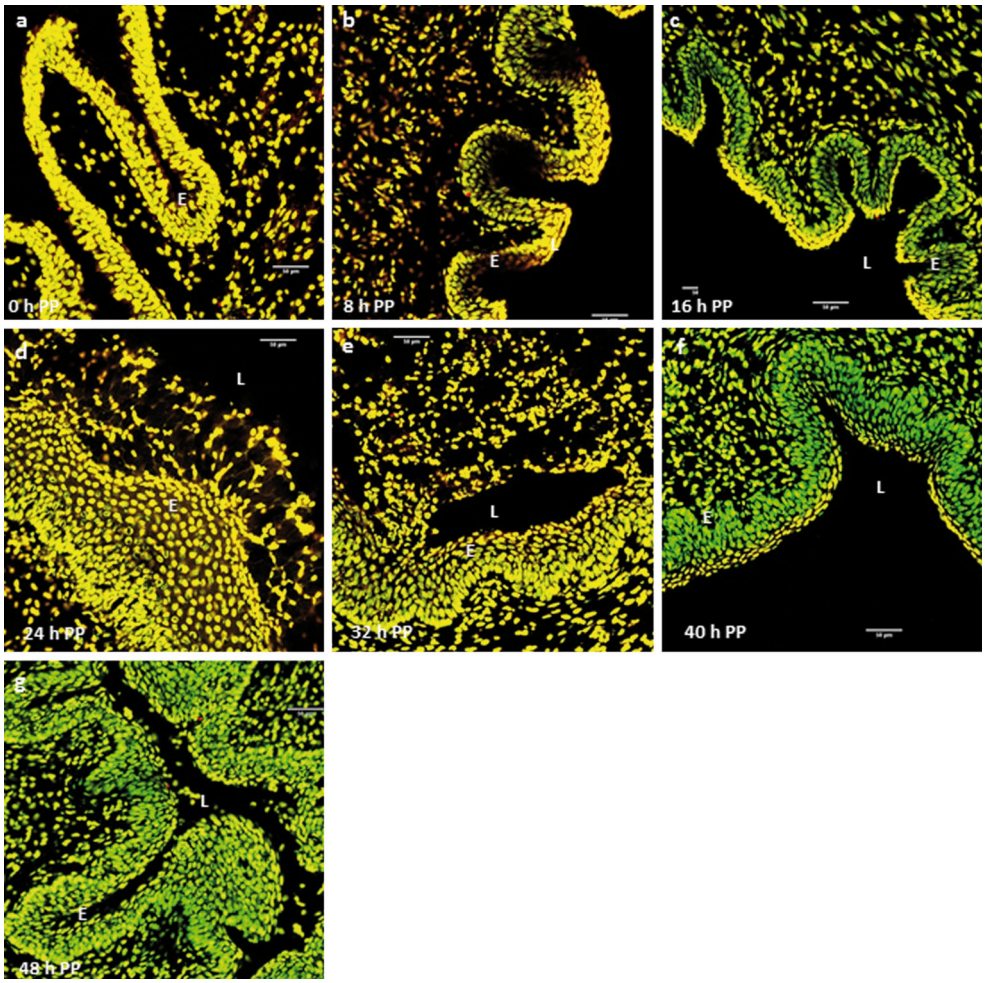

Fig. 6 Chronological cellular expression pattern of HIF-1α protein in postpartum (PP) mouse cervix, as revealed by confocal immunofluorescence. HIF-1α fluorescence was localized in all cell types, notably epithelial (*E*) and stromal cells, with a spike of expression at 8 h PP particularly in stromal cells (*red* fluorescence) and diminished at 16, 40 and the lowest expression by 48 h PP. The sections were stained with HIF-1α Texas red antibodies and a nuclei-specific stain, i.e., Sytox Green™, which stains *green*. A moderate overlap between the two appears as *yellow*, with a strong HIF-1α staining appearing as *red*. *L* lumen. $n=1$

interest, cervical tissue, as seen at low (×50) magnification, is clearly greater in size at 0 h compared to 48 h postpartum, which again is consistent with cell proliferation leading up to parturition, and postpartum recovery back to a non-pregnant state. The exact identity of the substance covering the epithelial cells, appearing at 24 h postpartum, is unclear. It is possible that it could be derived from ECM, cervical mucus, or cellular debris. These observations and suggestions are consistent with previous reports that suggest postpartum repair may involve both clearance and synthesis of ECM molecules (Timmons et al. 2010), which may explain why in the present study the substance was only seen at 24 h postpartum, but not at 0 and 48 h postpartum. Using H&E staining, we were able to see changes within the cervical epithelium, mucosa, and other intracellular structures, as well as the ECM. H&E staining studies also confirmed both the folded convoluted nature of the cervical epithelium at 0 h postpartum and the covering substance at 24 h postpartum, revealed by SEM. Also, the presence of cellular nuclei in the covering substance suggests that it could be cellular debris. However, it is also possible that there could be ECM molecules and/or cervical mucus in the covering substance.

We have previously characterized the expression profile of HIF-1α (preliminary data) as well as VEGF and its receptors, VEGFR-1 and VEGFR-2 (Mowa et al. 2004, 2008b; Donnelly et al. 2013) in pre-partum and 2 days postpartum rodent cervix. Here, we sought to determine their chronological expression profile postpartum at different time points between parturition and 48 h postpartum in order to determine whether they have a temporal relationship with and, ultimately, have a role in postpartum cervical repair. Of interest, levels of HIF-1α, VEGF, and VEGFR-1 (gene and protein) were found to be elevated in early postpartum and decreased to their lowest levels by 48 h postpartum, a pattern that was similar to the genome-wide expression pattern of proteins associated with pro-inflammatory and wound healing, revealed in our preliminary proteomics analysis (data not shown). Since HIF-1α is ultra-sensitive to changes in intracellular oxygen concentration, i.e., is rapidly degraded under normoxic conditions (Semenza 2004), but activated and stabilized under hypoxic conditions (Majmundar et al. 2010; Semenza 2004), its local tissue concentrations can therefore be used to indirectly measure the degree of local oxygen concentrations. Thus, elevated gene and protein expression of HIF-1α observed at 0 h

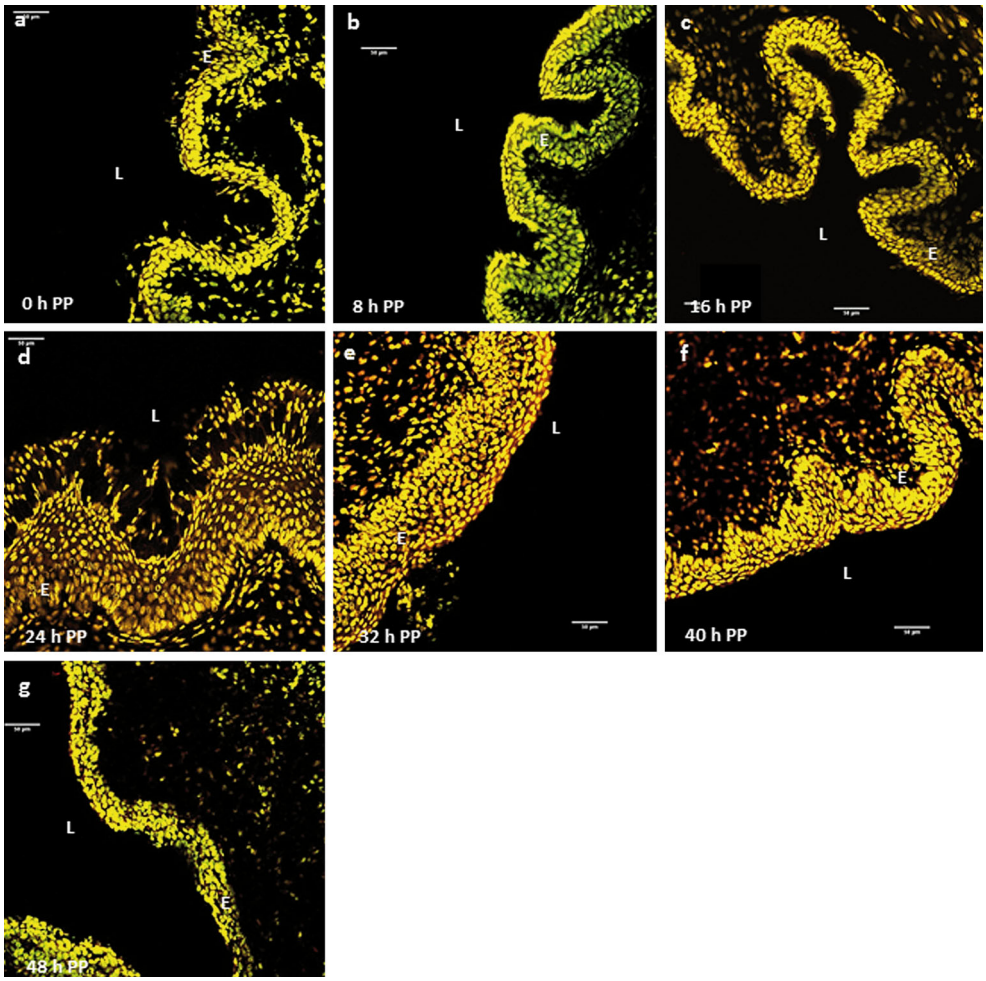

Fig. 7 Chronological cellular expression of Flt-1 protein in the postpartum mouse cervix, as revealed by confocal immunofluorescence. Overall, Flt-1 protein expression was diffusely localized in both the epithelial (*E*) and stromal cells stained. However, a more pronounced expression was largely localized in the epithelia, and overall, a weaker signal was observed in the cells between 40 and 48 h. The tissue was incubated with Flt-1 Texas red antibodies, and a nuclei-specific stain, i.e., Sytox Green™, which stains *green*. Any overlap between the two appears as *yellow*, with a strong Flt-1 appearing as *red*. *L* lumen. $n=1$

postpartum, in the cervix in the present study, suggests the presence of a hypoxic state. Under such conditions (hypoxic), HIF-1α, overall, induces transcription of a range of genes that promote angiogenesis and cell survival, notably VEGF, but also including: metabolic enzymes, cytokines, growth factors, cytoskeletal proteins, and ECM molecules (Majmundar et al. 2010; Semenza 2004). Indeed, HIF-1α is the most potent inducer of VEGF (Majmundar et al. 2010), the key angiogenic molecule, which is also intricately linked to inflammation in a variety of tissue types, including the cervix (Nguyen et al. 2012; Mowa et al. 2008b), as well as wound healing in general (Galiano et al. 2004; Mowa et al. 2008a; Alberts et al. 2008; Bao et al. 2009; Eming and Krieg 2006).

While the pattern of HIF-1α, VEGF, and VEGFR-1 gene/protein expressions were in agreement, it was not so with VEGFR-2 gene and protein expression. Real-time PCR demonstrated a decrease in mRNA expression of VEGFR-2 between 0 and 48 h postpartum. However, protein levels of VEGFR-2 steadily increased, peaking between 40 and 48 h postpartum, as revealed by both Western blot and confocal immunofluorescence. It is likely that the turnover of VEGFR-2 transcript is higher (more unstable) than protein. VEGFR-2 is known to mediate most biological effects of VEGF, including mitogenic, angiogenic, and cell survival properties (Ge et al. 2012), whereas, although VEGFR-1 has a higher affinity for VEGF, it has weak tyrosine phosphorylation activity compared to VEGFR-2 (Roskoski 2007), and, therefore, is of less functional significance. Further, the VEGFR-1 transcript can undergo alternative splicing that generates a soluble VEGFR-1 that acts to suppress the effects of VEGF (Roskoski 2007; Stuttfield and Ballmer-Hofer 2009). However, VEGFR-1 is known to play a role in cell migration (Roskoski 2007), and in certain cells that express VEGFR-1, such as blood platelets, macrophages, and neutrophils, and Flt-1 also mediates their chemotactic response to VEGF during wound healing (Bao et al. 2009; Eming and Krieg 2006). Based on these facts, and taking into account the difference of VEGF receptors in biochemical properties, it is likely that VEGFR-1 mediates VEGF processes associated with early hours of postpartum cervical repair, such as immune-related and wound-healing functions, while VEGFR-2 mediates the latter part of postpartum repair and VEGF, and perhaps functions such as cell survival and angiogenesis. Collectively, these processes restore

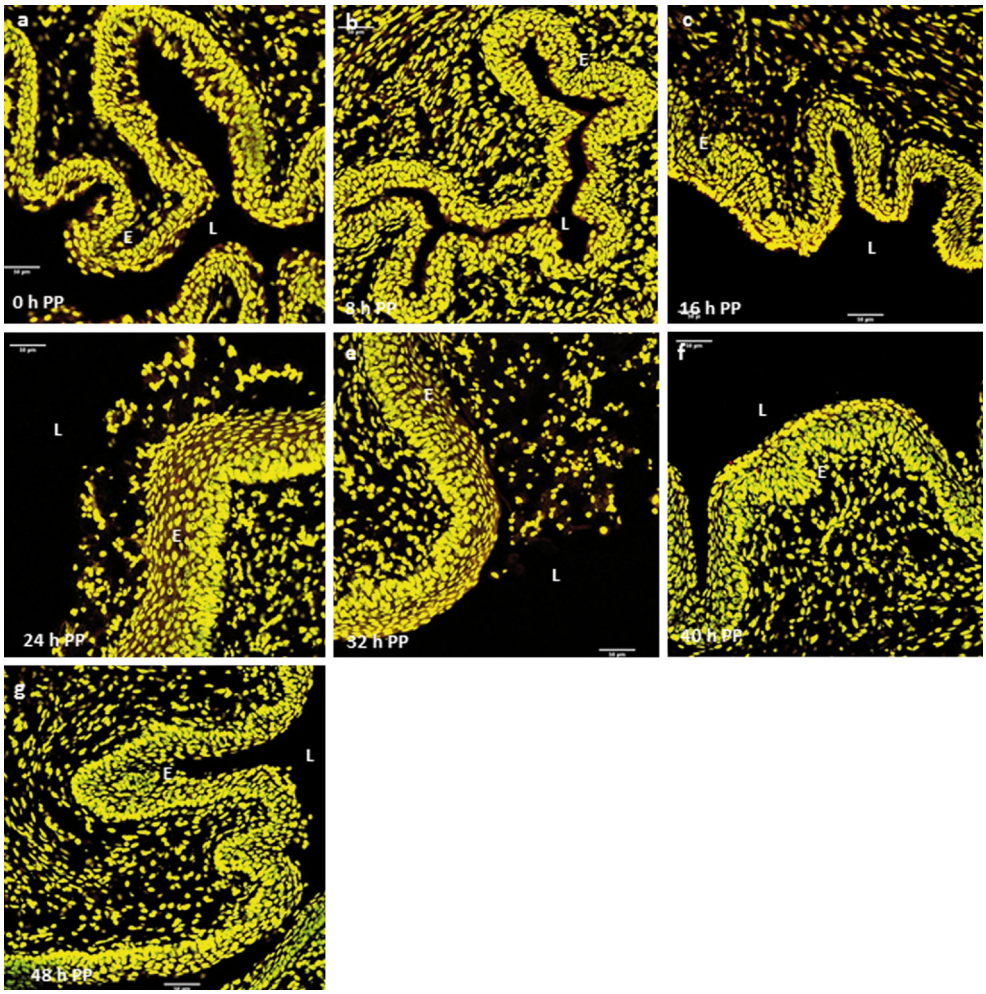

Fig. 8 Chronological cellular expression pattern of VEGFR-2 protein in the postpartum mouse cervix, as revealed by confocal immunofluorescence. Overall, the signal of VEGFR-2 staining increased over time, particularly from 16 h postpartum in epithelia (*E*) and stromal cells, with the weakest signal appearing between 0–8 h and slightly diminishing at 48 h. The tissue was incubated with VEGFR-2 Texas red antibodies, and a nuclei-specific stain, i.e., Sytox Green™, which stains *green*. Any overlap between the two appears as *yellow*, with a strong VEGFR-2 signal appearing as *red*. *L* lumen. $n=1$

the cervix back to its non-pregnant state. Future functional studies are needed to test these speculations.

Hypoxia is known to be involved in various physiological and/or pathological responses, but may also play a role in parturition. For instance, in the high altitude mountain ranges of the Andes, expectant mothers are believed to induce childbirth at term by climbing to high elevations with a lower oxygen environment or hypoxia. Similarly, it is likely that hypoxia could account for the increased risk in preterm labor associated with smoking. Interestingly, our recent preliminary proteomics data revealed two hypoxia-induced proteins that were highly expressed at 0 h postpartum. Transgelin is an actin-crosslinking protein known to be expressed in fibroblasts and smooth muscle (Kim et al. 2009, 2012), and is strongly expressed in both the uterus and cervix. Recent studies by Kim et al. (2012) demonstrated that transgelin is up-regulated by hypoxia, independent of HIF-1α, and also activates the insulin-like growth factor receptor 1 (IGFR1) signaling pathway under hypoxic stress. The IGFR1 pathway has recently been shown to promote cell survival under hypoxic stress (Kim et al. 2012; Gariboldi et al. 2010) by up-regulating HIF-1α gene transcription (Gariboldi et al. 2010) and stabilizing HIF-1α protein (Piecewicz et al. 2012). This up-regulation and stabilization of HIF-1α by the IGFR1 axis has been shown to induce VEGF expression during embryonic vasculogenesis (Piecewicz et al. 2012), and angiogenesis in malignant tumor cells under hypoxic stress (Gariboldi et al. 2010). Whether transgelin acts upstream of HIF-1α and VEGF in postpartum cervical repair is for now speculative. Like transgelin, vimentin has also been associated with hypoxia. For instance, it has been shown to redistribute among the endothelial cell into stable structures in response to hypoxia (Lui et al. 2010), is involved in general wound healing (Rogel et al. 2011), and is known to play a role in migrating cells, including fibroblasts, macrophages, endothelial cells, and invasive cancer cells (Lui et al. 2010; Rogel et al. 2011; Hefland et al. 2011; Glaser-Gabay et al. 2011). Further studies are needed to examine the roles of these hypoxia-induced proteins in the postpartum phase of cervical remodeling. Postpartum repair has been previously characterized as a proinflammatory and wound-healing process (Timmons and Mahendroo 2007; Bauer et al. 2009; Gonzalez et al. 2009). Our current data of postpartum cervical tissue are consistent with the earlier studies.

In summary, our data provide the first expression profile of VEGF, its receptors (Flt-1 and VEGFR-2), and HIF-1α and link their pattern of expression to hypoxia-related proteins and morphological changes. The limitation of the current study includes small sample size and lack of a detailed immunochemical evaluation of angiogenic factors, particularly markers of angiogenesis, such as endothelial markers.

Acknowledgment Funding for the present study was provided by the College of Arts and Sciences, Appalachian State University, Boone, NC, USA.

References

Alberts B, Johnson A, Lewis J, Raff M, Roberts K, Walter P (2008) Molecular biology of the cell. Garland Science, New York, pp 1417–1482

Bao P, Kodra A, Tomic-Canic M, Golinko MS, Ehrlich HP, Brem H (2009) The role of vascular endothelial growth factor in wound healing. J Surg Res 15:347–358

Bauer M, Mazza E, Jabareen M, Sultan L, Bajka M, Lang U, Zimmermann R, Holzapfel GA (2009) Assessment of the in vivo biomechanical properties of the human uterine cervix in pregnancy using the aspiration test a feasibility study. Eur J Obstet Gynecol 144S:S77–S81

Donnelly S, Nguyen BT, Rhyne S, Estes J, Jesmin S, Mowa CN (2013) Vascular endothelial growth factor induces growth of the uterine cervix and immune cell recruitment in mice. J Endocrinol 217:83–94

Eming SA, Krieg T (2006) Molecular mechanisms of VEGF-A action during tissue repair. J Invest Dermatol 11:79–86

Fahmy K, el-Gazar A, Sammour M, Nosair M, Salem A (1991) Postpartum colposcopy of the cervix injury and healing. Int J Gynaecol Obstet 34:133–137

Galiano RD, Tepper OM, Pelo CR, Bhatt KA, Callaghan M, Bastidas N, Bunting S, Steinmetz HG, Gurtner GC (2004) Topical vascular endothelial growth factor accelerates diabetic wound healing through increased angiogenesis and by mobilizing and recruiting bone marrow-derived cells. Am J Pathol 164:1935–1947

Gariboldi MB, Ravizza R, Monti E (2010) The IGFR1 inhibitor NVP-AEW541 disrupts a pro-survival and pro-angiogenic IGF-STAT3-HIF1 pathway in human glioblastoma cells. Biochem Pharmacol 80: 455–462

Ge X, Zhao L, He L, Chen W, Li X (2012) Vascular endothelial growth factor receptor 2 (VEGFR2, Flk-1/KDR) protects HEK293 cells against $CoCl_2$-induced hypoxic toxicity. Cell Biochem Funct 30:151–157

Glaser-Gabay L, Raiter A, Battler A, Hardy B (2011) Endothelial cell surface vimentin binding peptide induces angiogenesis under hypoxic/ischemic conditions. Microvasc Res 82:221–226

Gonzalez JM, Xu H, Chai J, Ofori E, Elovitz MA (2009) Preterm and term cervical ripening in CD1 mice (*Mus musculus*): similar or divergent molecular mechanisms? Biol Reprod 81:1226–1232

Hefland BT, Mendez MG, Murthy SN, Shumaker DK, Grin B, Mahammad S, Aebi U, Wedig T, Wu YI, Hahn KM, Inagaki M, Herrmann H, Goldman RD (2011) Vimentin organization modulates the formation of lamellipodia. Mol Biol Cell 22:1274–1289

Kim TR, Moon JH, Lee HM, Cho EW, Paik SG, Kim IG (2009) SM22alpha inhibits cell proliferation and protects against anticancer drugs and gamma-radiation in HepG2 cells: involvement of metallothioneins. FEBS Lett 583:3356–3362

Kim TR, Cho EW, Paik SG, Kim IG (2012) Hypoxia-induced SM22α in A549 cells activates the IGF1R/PI3K/Akt pathway, conferring cellular resistance against chemo-and radiation therapy. FEBS Lett 586:303–309

Lui T, Guevara OE, Warburton RR, Hill NS, Gaestel M, Kayyali US (2010) Regulation of vimentin intermediate filaments in endothelial cells by hypoxia. Am J Physiol Cell Physiol 299:C363–C373

Mahendroo M (2012) Cervical remodeling in term and preterm birth: insights from an animal model. Reproduction 143:429–438

Majmundar AJ, Wong WJ, Simon MC (2010) Hypoxia inducible factors and the response to hypoxic stress. Mol Cell 40:294–309

Mowa CN, Jesmin S, Sakuma I, Usip S, Togashi H, Yoshioka M, Hattori Y, Papka R (2004) Characterization of vascular endothelial growth factor (VEGF) in the uterine cervix over pregnancy: effects of denervation and implications for cervical ripening. J Histochem Cytochem 52:1665–1674

Mowa CN, Hoch R, Montavon CL, Jesmin S, Hindman G, Hou G (2008a) Estrogen enhances wound healing in the penis of rats. Biomed Res 29:267–270

Mowa CN, Li T, Jesmin S, Folkesson HG, Usip SE, Papka RE, Hou G (2008b) Delineation of VEGF-regulated genes and functions in the cervix of pregnant rodents by DNA microarray analysis. Reprod Biol Endocrinol 6:1–10

Nguyen BT, Minkiewicz V, McCabe E, Cecile J, Mowa CN (2012) Vascular endothelial growth factor induces mRNA expression of pro-inflammatory factors in the uterine cervix of mice. Biomed Res 33:363–372

Piecewicz SM, Pandey A, Roy B, Xiang SH, Zetter BR, Sengupta S (2012) Insulin-like growth factors promote vasculogenesis in embryonic stem cells. PLoS ONE 7:e32191

Read CP, Word RA, Ruschenisky MA, Timmons BC, Mahendroo M (2007) Cervical remodeling during pregnancy and parturition: molecular characterization of the softening phase in mice. Reproduction 134:327–340

Rogel MR, Soni PN, Troken JR, Sitikov A, Trejo HE, Ridge KM (2011) Vimentin is sufficient and required for wound repair and remodeling in alveolar epithelial cells. FASEB J 25:3873–3883

Roskoski R Jr (2007) Vascular endothelial growth factor (VEGF) signaling in tumor progression. Crit Rev Oncol Hematol 62:179–213

Semenza GL (2004) Hydroxylation of HIF-1: oxygen sensing at the molecular level. Physiology 19:176–182

Stuttfield E, Ballmer-Hofer K (2009) Structure and function of VEGF receptors. Life 6:915–922

Timmons BC, Mahendroo M (2007) Process regulating cervical ripening differ from cervical dilation and postpartum repair: insights from gene expression studies. Reprod Sci 14:53–62

Timmons BC, Fairhurst AM, Mahendroo M (2009) Temporal changes in myeloid cells in the cervix during pregnancy and parturition. J Immunol 182:2700–2707

Timmons BC, Akins M, Mahendroo M (2010) Cervical remodeling during pregnancy and parturition. Trends Endocrinol Metab 21:353–361

Word RA, Li XH, Hnat M, Carrick K (2007) Dynamics of cervical remodeling during pregnancy and parturition: mechanisms and current concepts. Semin Reprod Med 25:69–79